

Fast and Accurate UWB Radar Imaging using Hybrid of Kirchhoff Migration and Stolt's F-K Migration with Inverse Boundary Scattering Transform

Takuya Sakamoto*, Toru Sato,
Graduate School of Informatics
Kyoto University
Yoshida-Honmachi, Sakyo-ku
Kyoto 606-8501, Japan

Pascal Aubry, Alexander Yarovoy
Microwave Sensing, Signals and Systems
Delft University of Technology
Mekelweg 4, 2628 CD
Delft, the Netherlands

Abstract—A fast and accurate radar imaging algorithm is proposed that is a hybrid of the Kirchhoff migration and Stolt's frequency-wavenumber (F-K) migration. The latter is known as a fast imaging method in the F-K domain using the fast Fourier transform. Kirchhoff migration is reported to be more accurate than Stolt's F-K migration, but requires locating reflection points. For this reason, Kirchhoff migration must be processed in the time domain, which can be extremely time-consuming. This study overcomes this hurdle by combining these two algorithms by introducing the texture angle and the inverse boundary scattering transform. These two tools enable the location of a reflection point to be determined quickly for each pixel of a radar image. Using the estimated locations, radar signals are modified according to the Kirchhoff integral. Then Stolt's F-K migration is applied to the modified signals to obtain an accurate radar image. To demonstrate the performance of the proposed method, the conventional Kirchhoff migration, Stolt's F-K migration and the proposed method are applied to a measured dataset.

I. INTRODUCTION

Ultra wide-band (UWB) radar imaging has been of great importance in a variety of applications such as sensor networks [1], through-the-wall imaging [2], [3], breast tumor detection [4], and ground penetrating radars [5]. Among these, some applications such as security systems require both accuracy and speed in imaging processing. Zhuge et al. [6] proposed an accurate imaging algorithm based on the Kirchhoff integral, which can generate clearer images than a conventional delay-and-sum (DAS) migration. The Kirchhoff migration is computed in the time-domain, making imaging processing time-consuming. Because many imaging systems require real-time processing, this drawback hinders the use of the method in practice.

Stolt's F-K migration is known to be a fast imaging method, and has been used in many studies [7], [8], [9]. Because the method performs back-projection in the frequency-wavenumber (F-K) domain, Stolt's F-K migration is basically the same as DAS migration [10], apart from the fact that the edges of the data matrix are suppressed by a roll-off window in calculating the fast Fourier transform (FFT), which leads

to some information loss. Therefore, the imaging capability of Stolt's F-K migration can be worse than that of DAS migration.

To overcome these difficulties, this paper presents a new method whereby Kirchhoff migration and Stolt's F-K migration are combined. The problem to be solved is that Kirchhoff migration requires reflection-point locations for each pixel of the radar image, which prevents its use with Stolt's F-K migration because target reflection points are unknown. The target reflection points must be first calculated in the time domain, thereupon Stolt's F-K migration can be applied. To tackle this aspect, we introduce the texture angle and the inverse boundary scattering transform (IBST). Both then allow us to modify the signals in the time domain so that they follow the same form of the Kirchhoff integrand. Next, the modified signals are transformed to the F-K domain to be processed by Stolt's F-K migration. Because the calculation of the texture angle and the IBST are fast, these additional processes do not slow the computational speed of Stolt's F-K migration. The proposed method is demonstrated to be able to generate high-quality images. The performance of the proposed method is confirmed by applying conventional Kirchhoff migration, Stolt's F-K migration, and our proposed method to the scattering data of five different targets: a knife, laser measure, handgun, bottled water, and set of keys. The application results indicate the high-quality imaging capability of the proposed method.

II. SYSTEM MODEL

The measurement system consists of a transmitter and a receiver positioned in the $z = 0$ plane in the direction of x at a fixed separation $2d$. The midpoint between the transmitter and receiver is denoted $(X, Y, 0)$; hence, transmitter and receiver are located at $\mathbf{r}_1 = (X - d, Y, 0)$ and $\mathbf{r}_2 = (X + d, Y, 0)$, respectively. With the transmitter-receiver pair scanning at discrete intervals across a region of the $z = 0$ plane, UWB

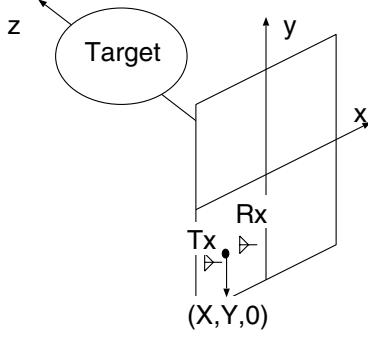


Fig. 1. System setup with antennas scanning from the x - y plane.

pulses are transmitted and pulse echoes are received. Figure 1 shows the system setup assumed in this paper.

The received signals contain not only echoes from the target but also a coupling signal propagating directly from the transmitter to the receiver. To eliminate this coupling signal, the background signal, measured without target prior to actual measurements, is subtracted from the received signal. Given the antennae midpoint $(X, Y, 0)$, the signal received is labeled $s(X, Y, Z)$, where $Z = ct/2$. Here, c is the speed of the electromagnetic wave and t the time interval between transmission and reception. Note that Z is not the z -component of the target, but a parameter to simplify the formulae introduced in the following sections.

III. STOLT'S F-K MIGRATION

Stolt's F-K migration is one of the fastest imaging algorithms using the FFT algorithm in the F-K domain. Let $\Phi(x, y, z, t)$ be a wavefield at a point (x, y, z) and time t , and $\phi(k_x, k_y, z, \omega)$ be the three-dimensional (3-D) Fourier transform in terms of x , y and t . This wavefield satisfies the Helmholtz equation

$$\nabla^2 \phi + k_0^2 \phi = 0, \quad (1)$$

which can be also written as

$$\frac{\partial^2}{\partial z^2} \phi + \hat{k}_z^2 \phi = 0, \quad (2)$$

where $k_0 = \omega/c$ and $\hat{k}_z = \sqrt{k_0^2 - k_x^2 - k_y^2}$, is the effective wavenumber in the z -direction, which assumes a plane wave. Equation (2) suggests that ϕ is approximated as a wave propagating in the z -direction with wavenumber \hat{k}_z .

If the wavefield is observed at all points in the x - y plane, i.e. $\Phi(x, y, 0, t)$ are known, the target image we need to estimate corresponds to $\Phi(x, y, z, 0)$; if the definition of $t = 0$ is suitably chosen, it can be expressed as

$$\Phi(x, y, z, 0) = \int \phi(k_x, k_y, 0, \omega) e^{j(k_x x + k_y y + \hat{k}_z z)} dk_x dk_y d\omega. \quad (3)$$

Expressing ω using \hat{k}_z as

$$\omega = c \cdot \text{sign}(\hat{k}_z) \sqrt{k_x^2 + k_y^2 + \hat{k}_z^2}, \quad (4)$$

Eq. (3) can be written as

$$\Phi(x, y, z, 0) = \int \frac{c \hat{k}_z}{\sqrt{k_x^2 + k_y^2 + \hat{k}_z^2}} \phi(k_x, k_y, 0, \omega) \cdot e^{j(k_x x + k_y y + \hat{k}_z z)} dk_x dk_y dk_z, \quad (5)$$

where the first term of the integrand is the Jacobian determinant arising from the change in variables from ω to \hat{k}_z . The important point is that Eq. (5) can be performed by applying the FFT to the re-sampled data $\frac{c \hat{k}_z}{\sqrt{k_x^2 + k_y^2 + \hat{k}_z^2}} \phi(k_x, k_y, 0, \omega(k_x, k_y, \hat{k}_z))$, where ω is explicitly shown as a function of k_x , k_y , and \hat{k}_z . Although using the FFT enables fast computation in executing Stolt's F-K migration, it is known that the imaging quality of the method is not as good as that from Kirchhoff migration.

IV. KIRCHHOFF MIGRATION

In a Dirichlet problem, the Kirchhoff integral is known to be an exact expression of a scalar wave field, which is used in Kirchhoff migration to generate high quality images. The Kirchhoff integral for a wave field $\Phi(\mathbf{r}, t) = \Phi(x, y, z, t)$ is expressed as

$$\Phi(\mathbf{r}, t) = \frac{1}{4\pi} \oint_S \left\{ \frac{\partial}{\partial R} \frac{\partial}{\partial n} \Phi(\mathbf{r}_1, t + \tau) - \frac{\partial}{\partial n} \frac{1}{R} \Phi(\mathbf{r}_1, t + \tau) + \frac{1}{cR} \frac{\partial R}{\partial n} \frac{\partial}{\partial t} \Phi(\mathbf{r}_1, t + \tau) \right\} dS, \quad (6)$$

where c is the speed of wave propagation, $\mathbf{r} = (x, y, z)$ is a point in a closed region bounded by surface S , $R = |\mathbf{r} - \mathbf{r}_1|$, $\tau = R/c$, and $\partial/\partial n$ means the spatial derivative in the direction of the normal vector to S . If surface information of the wave field is given, its value at \mathbf{r} is calculated using Eq. (6).

Considering the two-way paths of radar measurement and the Born approximation, Zhuge et al. [6] derived the following formula to obtain a radar image $I(\mathbf{r})$.

$$I(\mathbf{r}) = \int_{S_1} \int_{S_2} \frac{\partial R_1}{\partial n_1} \frac{\partial R_2}{\partial n_2} \frac{1}{R_1 R_2} \cdot \left\{ \frac{1}{c^2} \frac{\partial^2}{\partial t^2} s_0(\mathbf{r}_1, \mathbf{r}_2, t + \tau) + \frac{1}{c} \left(\frac{1}{R_1} + \frac{1}{R_2} \right) \frac{\partial}{\partial t} s_0(\mathbf{r}_1, \mathbf{r}_2, t + \tau) + \frac{1}{R_1 R_2} s_0(\mathbf{r}_1, \mathbf{r}_2, t + \tau) \right\} dS_1 dS_2 \Big|_{t=0}, \quad (7)$$

where \mathbf{r}_1 and \mathbf{r}_2 are the positions of the transmitter and receiver, $R_i = |\mathbf{r} - \mathbf{r}_i|$ ($i = 1, 2$), $\tau = (R_1 + R_2)/c$, and $\partial/\partial n_j$ ($j = 1, 2$) are the spatial derivatives normal to S_j . Therefore, the signal is also expressed as $s_0(\mathbf{r}_1, \mathbf{r}_2, t) = s(X, Y, Z)$ with $\mathbf{r}_1 = (X - d, Y, 0)$, $\mathbf{r}_2 = (X + d, Y, 0)$ and $Z = ct/2$.

Stolt's F-K migration cannot be used to calculate Eq. (7) because R_i , and $\partial R_i/\partial n_i$ ($i = 1, 2$) are unknown. As a result, one must perform a time-domain integral of Eq. (7) which is time-consuming and impractical in many applications. In the

next section, we overcome this difficulty with the introduction of two tools: IBST and texture angles.

V. INVERSE BOUNDARY SCATTERING TRANSFORM AND TEXTURE ANGLE

We have developed a fast radar imaging algorithm SEABED (an acronym for shape estimation algorithm based on the boundary scattering transform (BST) and extraction of directly scattered waves), which employs the IBST, which is a reversible transform between a target shape and the corresponding echo data [11], [12], [13], [14], [15]. Because the IBST describes one-to-one correspondence, the SEABED does not require any iterative or repetitive processing, making the imaging fast. Another advantage of the SEABED is that a target location is estimated for each pixel of a radar image, which cannot be done using other conventional methods. This characteristic is exploited in this study to develop a new algorithm.

A radar image can be obtained using the following IBST [16] applied to signal $s(X, Y, Z)$:

$$x = X - \frac{2Z^3 Z_X}{Z^2 - d^2 + \sqrt{(Z^2 - d^2)^2 + 4d^2 Z^2 Z_X^2}}, \quad (8)$$

$$y = Y + Z_Y \{d^2(x - X)^2 - Z^4\} / Z^3, \quad (9)$$

$$z = \sqrt{Z^2 - d^2 - (y - Y)^2 - \frac{(Z^2 - d^2)(x - X)^2}{Z^2}} \quad (10)$$

using for simplicity $Z_X = \partial Z / \partial X$ and $Z_Y = \partial Z / \partial Y$. In the original SEABED, signal peaks are extracted and the IBST is applied to only these peaks. However, in this study, we need to know the target location corresponding to all the pixels of a radar image.

We introduce the texture angle for radar images to estimate the derivatives Z_X and Z_Y required in Eqs. (8) and (9). The texture angle was originally proposed in estimating target speeds from radar signals [17]. We use the same concept for a different purpose; we define the texture angle of a radar signal $s(X, Y, Z)$ as

$$\theta_X(X, Y, Z) = \tan^{-1} \left(\frac{\partial s(X, Y, Z) / \partial X}{\partial s(X, Y, Z) / \partial Z} \right), \quad (11)$$

$$\theta_Y(X, Y, Z) = \tan^{-1} \left(\frac{\partial s(X, Y, Z) / \partial Y}{\partial s(X, Y, Z) / \partial Z} \right). \quad (12)$$

The derivatives Z_X and Z_Y needed in the IBST are estimated as $Z_X = \tan(\theta_X)$ and $Z_Y = \tan(\theta_Y)$. As a result, we can obtain the estimate of a target position (x, y, z) using Eqs. (8-10).

Next, the target position (x, y, z) is used to calculate

$$R_1 = \sqrt{(x - X + d)^2 + (y - Y)^2 + z^2}, \quad (13)$$

$$R_2 = \sqrt{(x - X - d)^2 + (y - Y)^2 + z^2} \quad (14)$$

and $\partial R_1 / \partial n_1 = z / R_1$, $\partial R_2 / \partial n_2 = z / R_2$. These values are substituted into the next equation to calculate a modified

Kirchhoff signal

$$s'_m(\mathbf{r}_1, \mathbf{r}_2, t) = \frac{\partial R_1}{\partial n_1} \frac{\partial R_2}{\partial n_2} \frac{1}{R_1 R_2} \cdot \left\{ \frac{1}{c^2} \frac{\partial^2}{\partial t^2} s(\mathbf{r}_1, \mathbf{r}_2, t) + \frac{1}{c} \left(\frac{1}{R_1} + \frac{1}{R_2} \right) \frac{\partial}{\partial t} s(\mathbf{r}_1, \mathbf{r}_2, t) + \frac{1}{R_1 R_2} s(\mathbf{r}_1, \mathbf{r}_2, t) \right\}. \quad (15)$$

Finally, as proposed in [6], the propagation path loss is compensated for using $s_m = R_1^2 R_2^2 s'_m$. Then the Kirchhoff migration can be rewritten as

$$I(\mathbf{r}) = \int_{S_1} \int_{S_2} s_m(\mathbf{r}_1, \mathbf{r}_2, (R_1 + R_2)/c) dS_1 dS_2, \quad (16)$$

which is a usual DAS migration, and can be performed using the FFT exactly as in Stolt's F-K migration. The use of the texture angle and IBST allows us to use both Stolt's F-K migration and Kirchhoff migration simultaneously, which means that we can obtain high-quality images within a short time.

VI. PERFORMANCE EVALUATION OF THE PROPOSED METHOD

In this section, we apply our proposed method to scattering datasets to study its performance. The datasets were measured in the frequency domain using a network analyzer (PNA E8364B, Agilent Technologies) sweeping 161 points at frequencies from 4.0 GHz to 20.0 GHz. Two Vivaldi antennas were used with $2d = 5.5$ cm antenna separation. The pair of antennas scan in the X - Y plane ($Z = 0$) from $X_{\min} \leq X \leq X_{\max}$ and $Y_{\min} \leq Y \leq Y_{\max}$ at intervals of $\Delta_{X,Y}$, where $\Delta_{X,Y} = 1.0$ cm and $X_{\min}, X_{\max}, Y_{\min}$ and Y_{\max} are -37.0, 37.0, -37.0 and 37.0 cm, respectively. Thus, the total number of measurement points is $75 \times 75 = 5625$. Figure 2 shows a flowchart of the antenna scanning procedure. The position $(X, Y, 0)$ is defined as the midpoint of the transmitting and receiving antennas, which are located at $(X + d, Y, 0)$ and $(X - d, Y, 0)$, where $d = 2.75$ cm. The transmitting power is 2.0 dBm. In our measurements, five targets (a knife, laser measure, handgun, bottled water, and keys) are fixed to a styrene foam board placed 60.0 cm from the antenna scanning plane (see Fig. 3). Note that the actual reflection points of these targets are not the same but spread over a range from 52.5 cm (the bottled water) and 59.5 cm (the keys).

Fig. 4 shows the signals received in the measurement for $X = -13$ cm. By incoherently integrating these unprocessed signals in terms of the delay path Z from $Z_1 = 52.5$ cm to $Z_2 = 59.5$ cm as

$$I_0 = \int_{Z_1}^{Z_2} |s(X, Y, Z)|^2 dZ, \quad (17)$$

we obtain the vague image shown in Fig. 5. Although the water bottle is just about visible in the bottom left, the unprocessed signals do not provide accurate information about the target shapes.

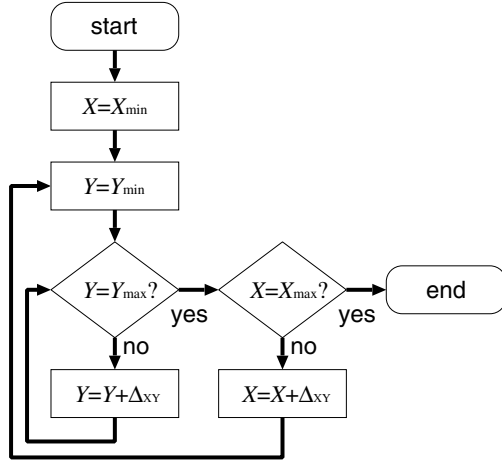


Fig. 2. Flowchart of the antenna scanning procedure.



Fig. 3. Photo of the five targets used in our measurement.

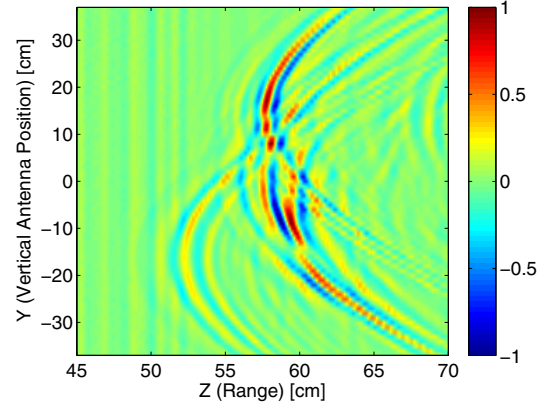


Fig. 4. Received raw signals for $X = -13$ cm.

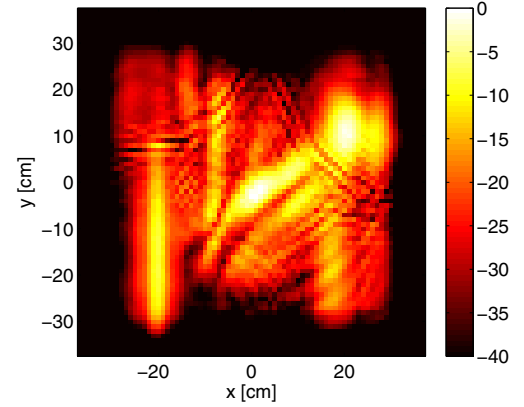


Fig. 5. Unprocessed data intensity corresponding to the targets' range (in dB).

Applying Eqs. (11) and (12) to the signals, the texture angle image is obtained (see Fig. 6). The gradient angle of the image is correctly estimated. Next, we use Eqs. (8), (9), and (10) to obtain target positions (x, y, z) for each pixel of the image. This enables us to calculate the modified Kirchhoff signals, as in Fig. 7. We see that higher frequency components are enhanced in this image compared with those of Fig. 4.

Finally, we apply Stolt's F-K migration to the modified Kirchhoff signals. We also apply conventional Kirchhoff migration, and Stolt's F-K migration for comparison. Figures 8 and 9 show the images generated using Stolt's F-K migration, and the proposed method, respectively. These images are normalized to the maximum pixel value. The image generated by the proposed method shows clearer details of the targets than the images produced by the conventional methods. This indicates the effectiveness of the proposed method for accurate imaging. To quantitatively investigate the images generated using different methods, we project radar images onto the x -axis (Fig. 10) to show sections of the target images given by Stolt's F-K migration, Kirchhoff migration and the proposed

method. The image produced by Kirchhoff migration is the sharpest, and the image generated using Stolt's F-K migration is not as focused as others. This result also shows that the image generated using the proposed method has a lower clutter level than that given by Stolt's F-K migration. It is an important future task to compare these methods with DAS migration as well to clarify their performances.

The computational times of Kirchhoff migration, Stolt's F-K migration, and the proposed method are 1148.8 s, 2.48 s, and 4.49 s, respectively. For this calculation, we used C language with SSL2 library (Fujitsu, Japan) running on a computer with an Intel Xeon E5-2650 v2 processor and 32 GB RAM. The speed of the proposed method is more than 250 times faster than the Kirchhoff migration, although Stolt's F-K migration is even 1.8 times faster than the proposed method. From this result, we can conclude that the computational speed of the proposed method is comparable to that of Stolt's F-K migration, whereas the proposed method can produce a clearer image than Stolt's F-K migration.

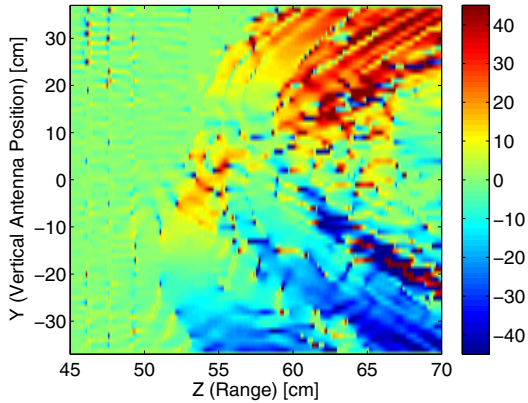


Fig. 6. Texture angle for the same data in Fig. 4 (in degrees).

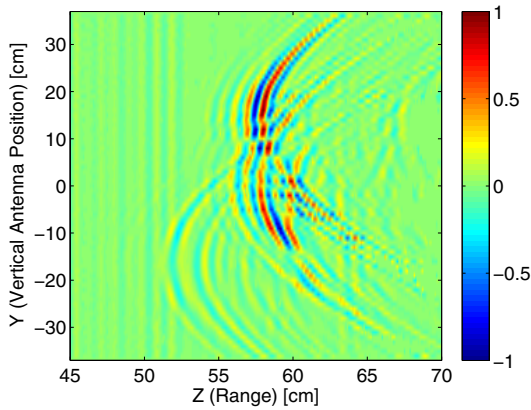


Fig. 7. Modified Kirchhoff signals for the same data in Fig. 4.

VII. CONCLUSION

In this paper, we proposed a fast and accurate imaging algorithm for UWB radar imaging, which combines Kirchhoff migration and Stolt's F-K migration. Kirchhoff migration requires the location of each reflection point of the target, thus preventing the use of Stolt's F-K migration for calculation. We introduced the texture angle and the IBST to obtain these locations, and generated the modified Kirchhoff signals, which correspond to the integrand of the Kirchhoff integral. Finally, we applied Stolt's F-K migration to the modified Kirchhoff signals to obtain an accurate radar image. The proposed method was applied to measured data from five different targets to demonstrate the effectiveness of the proposed method. We also evaluated the computational speeds of the four different imaging methods, to find that the proposed method is more than 250 times faster than the conventional Kirchhoff migration algorithms.

REFERENCES

[1] M. Arik, O. B. Akan, "Collaborative mobile target imaging in UWB wireless radar sensor networks," *IEEE Journal on Selected Areas in Communications*, vol. 28, no. 6, pp. 950–961, June, 2010.

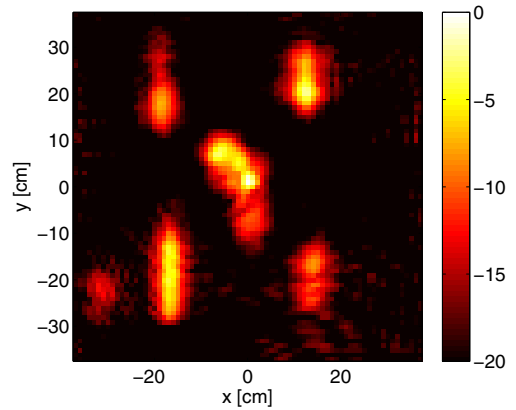


Fig. 8. Image generated using Stolt's F-K migration (in dB). Computational time was 2.48 s.

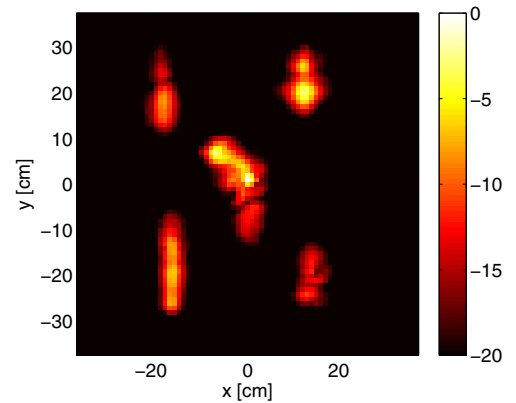


Fig. 9. Image generated using the proposed method (in dB). Computational time was 4.49 s.

[2] Y. Yang and A. E. Fathy, "Development and implementation of a real-time see-through-wall radar system based on FPGA," *IEEE Trans. Geoscience and Remote Sensing*, vol. 47, no. 5, pp. 1270–1280, May 2009.

[3] V. Venkatasubramanian, H. Leung, L. Xiaoxiang, "Chaos UWB Radar for Through-the-Wall Imaging," *IEEE Transactions on Image Processing*, vol. 18, no. 6, pp. 1255–1265, June 2009.

[4] H. F. Abutarboush, M. Klemm, "Signal Selection for Contrast-Enhanced UWB Microwave Radar Imaging With Inhomogeneous Breast Phantoms," *IEEE Antennas and Wireless Propagation Letters*, vol. 12, pp. 1408–1411, 2013.

[5] T. Counts, A. C. Gurbuz, W. R. Scott Jr., J. H. McClellan, and K. Kim, "Multistatic ground-penetrating radar experiments," *IEEE Trans. Geoscience and Remote Sensing*, vol. 45, no. 8, pp. 2544–2553, August 2007.

[6] X. Zhuge, A. G. Yarovoy, T. Savelyev, L. Ligthart, "Modified Kirchhoff migration for UWB MIMO array-based radar imaging," *IEEE Transactions on Geoscience and Remote Sensing*, vol. 48, no. 6, pp. 2692–2703, 2010.

[7] X. Xu, E. L. Miller, C. M. Rappaport, "Minimum entropy regularization in frequency-wavenumber migration to localize subsurface objects," *IEEE Transactions on Geoscience and Remote Sensing*, vol. 41, no. 8, pp. 1804–1812, August 2003.

[8] J.-G. Zhao, M. Sato, "Radar Polarimetry Analysis Applied to Single-Hole Fully Polarimetric Borehole Radar," *IEEE Transactions on Geoscience and Remote Sensing*, vol. 44, no. 12, pp. 3547–3554, December 2006.

[9] D. Garcia, L. L. Tarnec, S. Muth, E. Montagnon, J. Porée, G. Cloutier, "Stolt's f-k migration for plane wave ultrasound imaging," *IEEE Transactions on Ultrasonics, Ferroelectrics and Frequency Control*, vol. 60, no. 9,

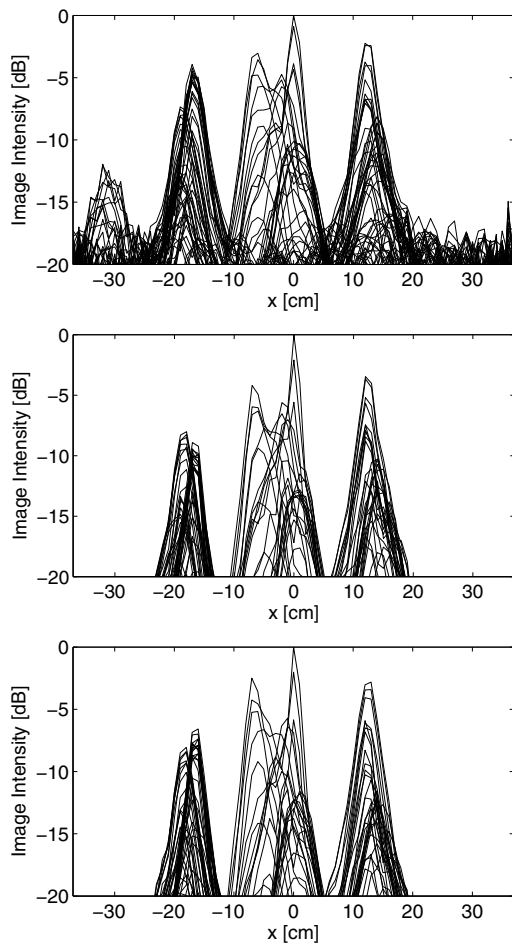


Fig. 10. Sections of the images generated using Stolt's F-K migration (top), Kirchhoff migration (middle), and the proposed method (bottom).

pp. 1853–1867, September 2013.

- [10] C. Gilmore, I. Jeffrey, and J. Lovetri, "Derivation and comparison of SAR and frequency-wavenumber migration within a common inverse scalar wave problem formulation," *IEEE Transactions on Geoscience and Remote Sensing*, vol. 44, no. 6, pp. 1454–1461, June 2006.
- [11] T. Sakamoto, "A fast algorithm for 3-dimensional imaging with UWB pulse radar systems," *IEICE Transactions on Communications*, vol. E90-B, no. 3, pp. 636–644, March 2007.
- [12] D. W. Winters, J. D. Shea, E. L. Madsen, G. R. Frank, B. D. Van Veen, S. C. Hagness, "Estimating the Breast Surface Using UWB Microwave Monostatic Backscatter Measurements," *IEEE Transactions on Biomedical Engineering*, vol. 55, no. 1, pp. 247–256, January 2008.
- [13] S. Hantscher, A. Reiszahn, C. G. Diskus, "Through-Wall Imaging With a 3-D UWB SAR Algorithm," *IEEE Signal Processing Letters*, vol. 15, pp. 269–272, February 2008.
- [14] R. Salman, I. Willms, "In-Wall Object Recognition based on SAR-like Imaging by UWB-Radar," *Proc. 8th European Conference on Synthetic Aperture Radar (EUSAR)*, June 2010.
- [15] S. Kidera, Y. Kani, T. Sakamoto, T. Sato, "A fast and high-resolution 3-D imaging algorithm with linear array antennas for UWB pulse radars," *IEICE Transactions on Communications*, vol. E91-B, no. 8, pp. 2683–2691, August 2008.
- [16] T. Sakamoto, T. G. Savelyev, P. J. Aubry, and A. G. Yarovoy, "Revised Range Point Migration Method for Rapid 3-D Imaging with UWB Radar," *Proc. 2012 IEEE International Symposium on Antennas and Propagation and USNC-URSI National Radio Science Meeting*, July 2012.
- [17] T. Sakamoto, T. Sato, Y. He, P. J. Aubry, A. G. Yarovoy, "Texture-based technique for separating echoes from people walking in UWB